Phase transitions of $Pb(Zr_xTi_{1-x})O_3$ ceramics

J. Frantti,[1,*] S. Ivanov,[2] S. Eriksson,[3] H. Rundlöf,[3] V. Lantto,[4] J. Lappalainen,[4] and M. Kakihana[1]
[1]*Materials and Structures Laboratory, Tokyo Institute of Technology, 4259 Nagatsuta, Midori-ku, Yokohama, 226-8503, Japan*
[2]*X-Ray Laboratory, Department of Inorganic Materials, Karpov Institute of Physical Chemistry, RU-103064 K-64, Moscow, Russia*
[3]*Studsvik Neutron Research Laboratory, Uppsala University, SE-611 82, Nyköping, Sweden*
[4]*Microelectronics and Materials Physics Laboratories, University of Oulu, Linnanmaa, P.O. Box 4500, FIN-90014 University of Oulu, Finland*

(Received 5 October 2001; revised manuscript received 7 June 2002; published 19 August 2002)

Recent experimental and theoretical reports on the structure of lead zirconate titanate [$Pb(Zr_xTi_{1-x})O_3$ (PZT)] ceramics with compositions in the vicinity of the morphotropic phase boundary are discussed. There has been ambiguity concerning the low-temperature structure of $x=0.52$ samples, due to the superlattice reflections which were not explained by the reported monoclinic phase Cm [B. Noheda, D. E. Cox, G. Shirane, R. Guo, B. Jones, and L. E. Cross, Phys. Rev. B **63**, 014103 (2001)]. Neutron powder diffraction (NPD) and Rietveld refinement were used to identify the space group symmetries of $x=0.52$ and $x=0.53$ samples at 10 K. Both samples had two coexisting phases $R3c$ and Cm at 10 K. At 10 K, monoclinic angles of both samples were larger than at 295 K, as was the octahedral tilt angle of the $R3c$ phase of the $x=0.53$ sample. We analyzed our previous and current NPD data to study the structural changes in PZT ceramics, $0.20 \leqslant x \leqslant 0.53$, as a function of x and temperature. Bond-valence calculations were carried out to test the models used in Rietveld refinements. Valences of Zr and Ti ions were larger and smaller than their nominal valences, respectively, although the anomaly decreased with increasing x. The composition-weighted-average valence of Zr and Ti ions was close to $+4$, and the relationship between the positions and valences of Zr and Ti ions explains the main structural features of PZT ceramics as a function of x. The valence of Pb ions was slightly below $+2$ and decreased with increasing x until it started to slightly increase for $x \geqslant 0.50$. Average oxygen valency was found to be close to -2. Also spontaneous polarization values were computed and found to be reasonable.

DOI: 10.1103/PhysRevB.66.064108 PACS number(s): 77.84.Dy, 61.12.Ld, 61.50.Ah, 81.30.Dz

I. INTRODUCTION

The structural details of lead zirconate titanate ($Pb(Zr_xTi_{1-x})O_3$, PZT) ceramics, especially close to the morphotropic phase boundary (MPB, corresponding to $x \approx 0.52$), have been keenly studied during the last few years. Particularly the recently reported phase transition between the tetragonal $P4mm$ and monoclinic Cm phases has gained the attention of experimentalists[1–9] and theorists.[10,11] Distortions related to this phase transition are small, and one needs high-quality samples and very careful data analysis procedures to quantify them. The phase transition is further obscured by the fact that PZT within these compositions does not have unambiguous space group symmetry. This is seen from Raman spectra, which clearly show that the local symmetry in PZT is lowered from the average symmetry far before the reported phase transition[5,7] at around $x \approx 0.50$.

At low temperature, PZT samples with $0.50 \leqslant x \leqslant 0.54$ contain two coexisting phases, and our opinion is that single-phase samples within this composition region have not been produced (there are different views, such as the ''one phase +diffuse scattering model'' for the room-temperature data[2,3]). This has obviously caused obstacles to model the behavior of these materials. For example, it is questionable if PZT is a good system to test the validity of the recently developed extension of Devonshire theory.[10] One of the crucial questions is whether the Cm phase is thermodynamically stable state when composition fluctuation is absent, as is discussed on the basis of the current neutron powder diffraction (NPD) data.

Space groups previously reported to correspond to the various phases of PZT ceramics are discussed in Sec. III. We also discuss the case of space groups, which one should consider while analyzing the diffraction and Raman scattering data (which often yield contradictory information in a case of PZT).

There are numerous symmetries practically indistinguishable by diffraction methods, when $x \approx 0.50$. Although one may argue that in a case that several space groups give essentially the same statistical figures of merit (e.g., residuals) and the instrumental resolution is not sufficient to rule out small distortions (resulting in overlapping Bragg reflection peaks), one should use the highest-symmetry space group, there are other factors to be considered. First, the results obtained from other experimental methods, such as spectroscopic methods, should be consistent with the space group symmetry. Second, it is often energetically favorable to transform via intermediate phase(s) (by symmetry, the phase transition $P4mm \rightarrow R3m$ has to be first order). For example, the space group Cm is a common subgroup of the phases $R3m$ and $P4mm$ according to the cascades $P4mm \rightarrow Cmm2 \rightarrow Cm$ and $R3m \rightarrow Cm$. This is analogous to the case of $(Na_{1-x}K_x)_{0.5}Bi_{0.5}TiO_3$ ceramics, reported in Ref. 12, where an intermediate phase (possibly tetragonal) was assumed to work as a bridge between the rhombohedral $R3c$ and tetragonal $P4bm$ phases, or to the case where the phase transition between the $R3c$ and $Pnma$ phases of relaxor $Na_{0.5}Bi_{0.5}TiO_3$ occurs via an intermediate phase.[13] Although the above-mentioned group-subgroup relation suggests a possibility that one has the $Cmm2$ phase as an intermediate

phase in PZT ceramics, to make a distinction between the $Cmm2$ and Cm symmetries is practically impossible to do by diffraction techniques, when $\beta \approx 90°$. In this article, we give the most plausible space groups for PZT ceramics at different temperatures and for different compositions. This analysis is based on careful study of the NPD patterns.

In Sec. IV, we review the recent NPD and synchrotron x-ray powder diffraction studies of PZT samples, and present new refinements for the $x=0.52$ sample at 10 K and for the $x=0.53$ sample at 10 K and at 295 K, which give an explanation for the superlattice reflection observed at low temperature. In this context, one cannot overestimate the importance of whole-pattern-fitting structure refinement, instead of studying just some selected peaks, for the correct space group determination. In Sec. IV C we show that composition fluctuation gives phase fraction and phase boundary location estimates consistent with the values extracted from the present NPD data.

Attention is also paid to distortions due to Zr substitution for Ti and/or temperature decrease. Both are crucial once one tries to understand the symmetries of PZT ceramics and the underlying reasons. This is the subject of Sec. V. It is shown in Sec. VI that the given structural models are capable of yielding reasonable values for spontaneous polarization.

In Sec. VII we present bond-valence calculations (BVC's) for our NPD data. This serves as a way to put local and average symmetry viewpoints together and, more importantly, serves as a way to test the observed structural parameters by allowing a comparison between the nominal valences and valences obtained by applying the BVC method for the model structures.

Finally, Sec. VIII discusses the relationship between the structural features and electrical properties.

II. EXPERIMENT

Preparation of ceramic $Pb(Zr_xTi_{1-x})O_3$ samples with $0.10 \leqslant x \leqslant 0.80$ via a solid-state reaction (sintering at a Pb-rich atmosphere) is described in our previous articles.[5–7] In a first step, pellets were pressed, after which surface layers were removed and pellets were ground into powder form. For NPD measurements PZT powders were put into a vanadium can.

Constant-wavelength NPD data were measured at the Studsvik Neutron Research Laboratory using a Huber two-circle diffractometer with an array of 35 ^{3}He detectors. Data were collected at room temperature (295 K) and at 10 K. After passing the neutron flux through the double monochromator, which consisted of two copper crystals in the (220) mode, the wavelength was 1.470(1) Å. The 2θ range measured was from 4.00° to 139.92° with a step size of 0.08° and the scanning time was 12 h. We also refer to the POLARIS time-of-flight neutron powder diffraction instrument at ISIS at the Rutherford Appleton Laboratory. For more details, see Ref. 6. Rietveld refinements were carried out using the general structure analysis system (GSAS).[14]

III. SPACE GROUP SYMMETRIES RELATED TO PZT CERAMICS

In this section, we discuss the space groups experimentally verified to correspond to PZT ceramics and, additionally, various subgroups of the cubic space group $Pm\bar{3}m$. The space groups described here are rhombohedral $R3m$ and $R3c$, tetragonal $P4mm$, orthorhombic $Pmm2$ and $Cmm2$, and monoclinic Pm and Cm. They are all subgroups of the space group $Pm\bar{3}m$. Closely related subgroups $P4/mmm$, $R\bar{3}m$, and $R\bar{3}c$ are not expected to correspond to the experimental data, as the previously reported second-harmonic generation measurements carried out for the $x=0.20,0.50,0.54$ samples[15] indicate that the only phase having inversion symmetry is the high-temperature cubic phase (temperatures where the inversion symmetry was lost in these samples were actually slightly higher than the ones reported in Ref. 16).

A. Rhombohedral space groups $R3m$ and $R3c$

Two rhombohedral phases, space groups $R3m$ (often referred to as $F_{R(HT)}$) and $R3c$ ($F_{R(LT)}$), are known to occur in Zr-rich PZT ceramics, depending on x and temperature (see, e.g., the phase diagram in Ref. 16, p. 136). The essential difference between the space groups $R3m$ and its subgroup $R3c$ is that the primitive cell is doubled in a phase transition $R3m \rightarrow R3c$. This primitive cell doubling is due to the rotation of oxygen octahedra around the threefold axis so that the adjacent oxygen octahedra are tilt with respect to each other along the hexagonal c axis. This can also seen by considering the fact that the three mirror planes m of the rhombohedral space group $R3m$ are replaced by three glide reflections (with a glide vector $\frac{1}{2}\mathbf{c}$) c in a space group $R3c$.

B. Space groups $P4mm$, $Pbam$, $Pmm2$, and $Cmm2$

Titanium-rich PZT ($x<0.50$) ceramics are traditionally considered to be tetragonal,[16] with space group $P4mm$.

The space group of antiferroelectric $PbZrO_3$ is $Pbam$,[17,18] and there are eight formula units per primitive cell, and is the only reported orthorhombic phase for bulk PZT (PZT having x close to unity is considered to have this space group symmetry), to our knowledge. There are older reports (see the early report by Jona *et al.*[19]), which assign a different space group for this orthorhombic phase, but the space group $Pbam$ seems now to be the generally accepted symmetry for these compositions.

In order to obtain the $Pmm2$ symmetry from its supergroup $P4mm$, ions have to be shifted so that crystal axes $a \neq b \neq c \neq a$ but there is no rotation of axes. Similarly, the space group $Cmm2$ is obtained if ions are shifted from their tetragonal positions so that the crystal axis $a \neq b \neq c \neq a$ and a and b axes are rotated by 45°.

C. Monoclinic space groups Pm and Cm

If, in addition to the changes which led to the space group $Pmm2$, the c axis is tilted so that $\alpha=\gamma=90° \neq \beta$, we end up with the space group Pm. Now, the fourfold and twofold rotation axes and three mirror planes are lost, so that the only remaining symmetry plane is σ_v, determined by the monoclinic a and c axes.

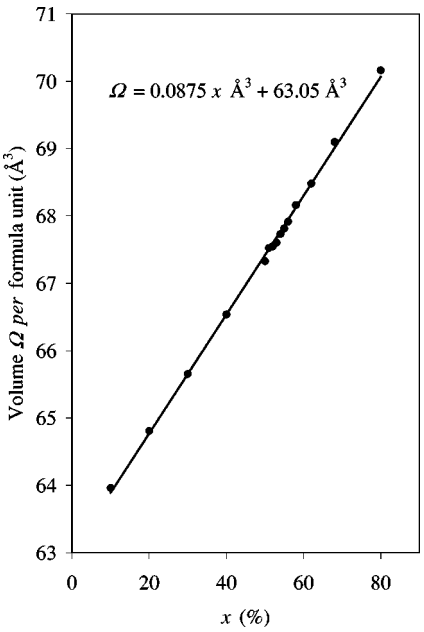

FIG. 1. The volume per formula unit ABO_3, Ω, in PZT ceramics, as a function of x.

Correspondingly, the space group Cm is obtained from the space group $Cmm2$ by tilting the c axis so that $\alpha=\gamma=90°\neq\beta$. The remaining mirror plane is σ_d. In the case of both monoclinic phases, symmetry requires that spontaneous polarization be in a mirror plane.

IV. NEUTRON AND SYNCHROTRON X-RAY POWDER DIFFRACTION RESULTS

Recently, Noheda *et al.*[1–3] used synchrotron radiation to study the symmetry of PZT disks as a function of Zr content and temperature. The synchrotron radiation they used had a resolution comparable to the high-resolution neutron powder diffractometer (HRPD) facility at ISIS (Rutherford Appleton laboratory). However, it has some drawbacks, when compared to the NPD facilities. First, it is more sensitive to texture effects, particularly, if the samples are disks.[3] To avoid this problem, Noheda *et al.* also used Debye-Scherrer geometry,[2] with a slightly lower resolution. Second, the different signs of the neutron scattering lengths (negative for Ti and positive for Zr) offer the possibility to determine the positions of these ions more reliably. As a third advantage, thermal displacement parameters can be refined more precisely using neutrons instead of x rays. Finally, as discussed below in the context of observing and identifying rhombohedral phases, NPD is better suited for the determination of oxygen positions, which is essential for the study of oxygen octahedral tilt. Figure 1 shows the volume per formula unit, Ω, for PZT ceramics in a composition range $0.10\leqslant x\leqslant 0.80$. Data were obtained from our samples. NPD data, when available, were used to compute Ω. Otherwise, x-ray diffraction data were used.

A. Ti-rich PZT powders

The noticable point necessitating further studies is whether the phase transition $P4mm\rightarrow Cm$ occurs via an orthorhombic phase, as Raman results suggest.[5,7] There are also two orthorhombic phases one should take into account, $Pmm2$ (B_1 strain) and $Cmm2$ (B_2 strain); see also Ref. 20. Further, it is also interesting to consider why the monoclinic phase has Cm symmetry, instead of Pm symmetry, which is shortly discussed at the end of the Sec. VII.

Experimentally, the distinction between the reported monoclinic symmetry Cm with β close to 90° (corresponding to PZT ceramics having $x\approx 0.50$ at low temperatures) and the $Cmm2$ symmetry or even $Pmm2$ symmetry is very difficult, particularly in the case of disordered solid solutions. Also in a case of $x<0.50$ samples it is not clear whether an orthorhombic distortion exists or not. Our NPD data[6] indicated that within standard errors the room-temperature symmetry of PZT powders with $x<0.50$ is $P4mm$. However, previously reported Raman results[5,7] give support to the orthorhombic phase with one formula unit per primitive cell, as it corresponds to 12 Raman-active modes (already in the case of the $x=0.10$ sample at 20 K). As the intensities of the peaks due to the splitting of the E-symmetry modes were roughly equal, one may think that instead of the symmetry $P4mm$ one should use orthorhombic symmetry (such as $Cmm2$, according to the phase transformation sequence $P4mm\rightarrow Cmm2\rightarrow Cm$). The origin of this peak split is not clear, which obscures the decision whether there is an orthorhombic distortion or not. On the other hand, previous refinements[6] indicated that Pb ions are shifted to the $\langle 110\rangle$ direction already when $x=0.20$, which favors $Cmm2$ symmetry.

Noheda *et al.*[3] studied the phase transition $Pm\bar{3}m\rightarrow P4mm$ and, further, to the Cm phase for various samples and temperatures. They reported a large coexistence region of the $P4mm$ and Cm phases as a function of temperature and, to a lesser extent, as a function of x. Although this type of phase coexistence is typically indicative of a first-order phase transition, the behavior of the monoclinic angle β supports a continuous phase transition (see Ref. 3). However, this is not easy to justify from the diffraction data, as it is not possible to identify the phases and phase symmetries unambiguously (see Figs. 4 and 5 in Ref. 3, and the discussion in Ref. 6). Obviously, extremely homogeneous samples could settle the disputes related to the phase diagram.

B. Samples with $x=0.52$ and $x=0.53$

Previously, we modeled $x=0.52$ sample using coexisting Cm and $P4mm$ phases, which gave an acceptable fit at room temperature.[21] However, there were several weak but observable reflections at 10 K, and at 10 K a better modeling was achieved by using $R3c$ as a symmetry for the secondary phase, together with the Cm phase. This was supported by low-temperature transmission electron microscopy and electron diffraction studies by Noheda:[22] they observed superlattice reflections which they first assigned to the $R3c$ symmetry and more recently to the Cc symmetry.[23] $R3c$ symmetry was confirmed by our HRPD data.[24] This is understandable by extrapolating the phase boundary limiting the $R3c$ phase down to lower temperatures (see phase diagram in Ref. 16).

TABLE I. Refinement results for the $x=0.52$ and $x=0.53$ samples. Data were collected using the NPD facility at Studsvik. Lattice parameters and fractional coordinates of the $R3c$ phase refer to the hexagonal setting. During the refinements, either the Pb ion (space group Cm) or Zr/Ti ions (space group $R3c$) were fixed to the origin. Numerical criteria for the $x=0.52$ sample were $\chi^2=2.280$, $R_{wp}=5.77\%$, $R_{wpb}=5.45\%$, $R_p=4.43\%$, $R_{pb}=4.24\%$ and for the $x=0.53$ sample they were $\chi^2=1.895$, $R_{wp}=5.89\%$, $R_{wpb}=5.49\%$, $R_p=4.56\%$, $R_{pb}=4.48\%$ (295 K) and $\chi^2=2.013$, $R_{wp}=6.20\%$, $R_{wpb}=5.75\%$, $R_p=4.72\%$, $R_{pb}=4.49\%$ (10 K).

x	0.52	0.52	0.53	0.53	0.53	0.53
T (K)	10	10	295	295	10	10
Space group	Cm	$R3c$	Cm	$R3c$	Cm	$R3c$
a (Å)	5.7097(7)	5.7437(17)	5.7244(18)	5.7504(8)	5.7253(10)	5.7400(7)
b (Å)	5.6984(7)		5.7165(17)		5.7075(8)	
c (Å)	4.136 66(26)	14.212(8)	4.1279(4)	14.195(4)	4.1205(5)	14.1985(32)
β (deg)	90.449(8)		90.289(21)		90.531(13)	
U_{iso}(Pb) (Å^2)	0.0090(12)	0.004(6)	0.0185(22)	0.030(6)	0.0087(19)	0.011(4)
U_{iso}(Ti,Zr) (Å^2)	0.0006(20)	0.0006(20)	0.0006(27)	0.0006(27)	0.0006(20)	0.0006(20)
U_{iso}(O_1) (Å^2)	0.0109(16)		0.0142(28)		0.0096(25)	0.0109(9)
U_{iso}($O_{2,3}$) (Å^2)	0.0131(12)	0.007(5)	0.0151(20)	0.024(4)	0.0122(18)	
z(Pb)		0.282(5)		0.2711(24)		0.2722(24)
x(Zr/Ti)	0.4607(26)		0.458(4)		0.459(4)	
z(Zr/Ti)	0.5590(26)		0.552(4)		0.557(4)	
x(O_1)	0.4602(14)		0.4721(30)		0.4538(21)	
z(O_1)	0.0924(15)		0.0848(23)		0.0850(23)	
x($O_{2,3}$)	0.2167(13)	0.1478(28)	0.2247(27)	0.1667(35)	0.2111(20)	0.1488(17)
y($O_{2,3}$)	0.2467(10)	0.3543(32)	0.2486(20)	0.3474(21)	0.2476(14)	0.3482(20)
z($O_{2,3}$)	0.6119(12)	0.081(6)	0.6048(20)	0.075(4)	0.6069(19)	0.0719(30)
Weight fraction (%)	87	13	68	32	71	29

The presence of the $R3c$ phase was most convincingly seen from the Bragg reflections not explainable by the Cm or the $P4mm$ phase.

This phase symmetry determination is discussed below in detail in the case of the $x=0.53$ sample. The structural data for these samples are shown in Table I. The room-temperature structure of the $x=0.52$ sample was previously studied,[21] and details of the Cm phase are given in Table VI, below. Figures 2 and 3 show the observed and calculated NPD profiles of the $Pb(Zr_{0.53}Ti_{0.47})O_3$ sample, collected at 295 K and at 10 K, respectively. We modeled both the room- and low-temperature structures using two coexisting phases $R3c$ and Cm, resulting in the weight fractions indicated in Table I.

One noticable point is that thermal displacement parameters are small. This is a well-known problem and is due to the fact that Zr and Ti ions do not have the same fractional coordinates (see, e.g., Refs. 2, 6, and 26 and Sec. VII A). For simplicity, for these two-phase structures we used the constraint that Zr and Ti ions have the same coordinates in each phase. This simplification did not affect the space group determination. Although it is common to refine occupancies, after several attempts we decided to use nominal occupancies and compute BVC and $\mathbf{P}_s$ to test the validity of the models. Refinement of occupancies did not essentially ''correct'' the thermal displacement parameters. Our trials for $x=0.20,0.30,0.40,0.50$ samples at 295 K and $x=0.53$ sample at 10 K indicated values well consistent with the nominal occupancies (the difference was typically less than 0.01). However, the occupancies of the secondary phases ($P4mm$ and $R3c$, respectively, for $x=0.52$ and $x=0.53$ samples) at 295 K differed significantly from the occupancies at 10 K. This is not physically meaningful, as it would mean significant and reversible diffusion of Zr and Ti at the *B*-cation sites. Further, as is discussed in Sec. VII, use of nominal composition values for x led to average valence values consistent with the nominal valences and also the condition set by the charge neutrality was well obeyed.

The low-temperature data were particularly interesting, as they showed that this sample contains also an $R3c$ phase, in addition to the Cm phase (see Fig. 3). Further, by studying the reflection $d_{1\bar{2}\bar{3}}\approx 2.44$ Å (corresponding to $2\theta\approx 34.9°$, when the wavelength is 1.4700 Å) and the four reflections $d_{4\bar{5}\bar{3}}=d_{1\bar{5}\bar{5}}$, $d_{3\bar{5}\bar{5}}$, $d_{2\bar{4}\bar{9}}$, and $d_{2\bar{3}\bar{11}}$ (indexed using the hexagonal setting) at $d\approx 1.06$ Å (corresponding to $2\theta\approx 87.8°$) it was possible not only to show the presence of the rhombohedral phase, but that these reflections correspond to the $R3c$ phase. In the case of the space groups Cm, $P4mm$, and $R3m$ (the other serious candidates to be considered; see also Ref. 27 concerning the recently reported Pc and Cc symmetries) there are no reflections in this regime. In addition, this model explains also the intensity between the monoclinic (220) and (002) reflections (at $2\theta\approx 42°$ in Figs. 2 and 3), which has been modeled using the cubic phase[2] and was assumed to be due to the tetragonal twin boundaries.[3] By putting the parameter e zero, using the notation defined by

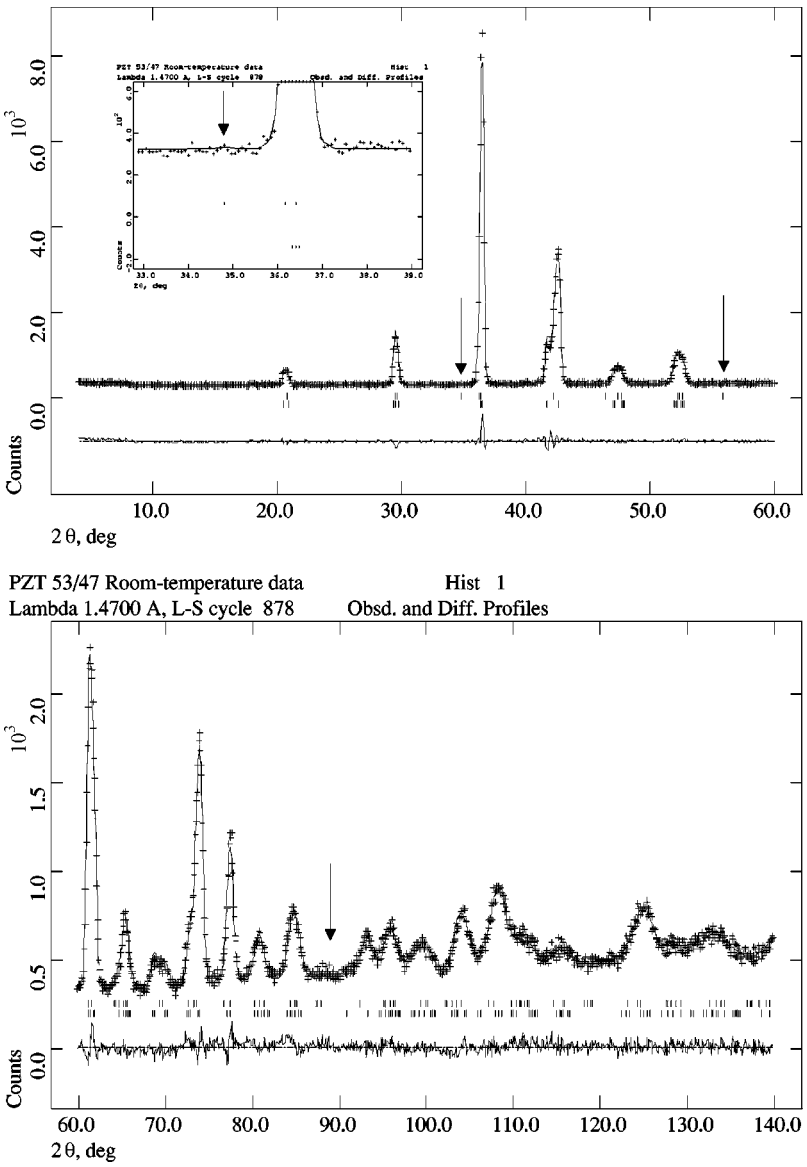

FIG. 2. Observed and calculated constant wavelength NPD (Studsvik) profile and its difference curves for a $Pb(Zr_{0.53}Ti_{0.47})O_3$ sample at 295 K. Top: small-2θ region. Bottom: large-2θ region. Peaks allowing the identification of the $R3c$ phase are indicated by arrows. The intensities of the peaks at around 35° (see inset) and 56° are zero, but the peak at around 88° has weak but nonvanishing intensity, indicating nonzero octahedral tilt. The tick marks shown, from up to down, correspond to the Bragg reflections from the $R3c$ and Cm phases, respectively.

Megaw and Darlington[25] (see also Ref. 26 and Table II), which tabulates the fractional coordinates using these parameters (this notation allows an easy comparison with the previously published data), and transforming the hexagonal axes $\mathbf{a}'$, $\mathbf{b}'$, and $\mathbf{c}'$ of the $R3c$ phase using the relations $\mathbf{a}'=-\mathbf{a}$, $\mathbf{b}'=-\mathbf{b}$, and $\mathbf{c}'=2\mathbf{c}$, one obtains the $R3m$ phase. This corresponds to the prohibition of the octahedral tilt and disappearance of the reflections at $d=2.44$ Å and at $d=1.06$ Å. Thus, these reflections are particularly informative and offer valuable information for the space group determination (and for the study of the octahedral tilt as a function of x and temperature). We did not force the space group symmetry to be $R3m$ but used the space group $R3c$ also in the case of the 295 K data and studied if the octahedral tilt ω is really decreased as temperature is increased from 10 K to 295 K. This was observed to be the case; see Table III. This significant decrease in tilt angle was also accompanied by the disappearance of the superlattice reflection at $d\approx 2.44$ Å (see the inset in Fig. 2), which indicates that the symmetry has nearly increased to $R3m$. However, as this transition seems to occur in a continuous manner and as we currently have only data collected at 295 K and at 10 K, it is not possible to say at which temperature the symmetry increases to $R3m$.

Finally, to understand the at first sight contradictory results concerning the one-phase versus two-phase models and space group assignments for the low-temperature phase given in the literature we simulated diffraction patterns. The possibility that the second phase has monoclinic Cc symmetry was also studied. Space group Cc is a subgroup of the space group $R3c$, and is capable of explaining the same reflections as the phase $R3c$. However, it predicts additional peak split and reflections at $d\approx 4.68$ Å, which were not observed in our constant-wavelength data. This was confirmed by studying the $Pb(Zr_{0.54}Ti_{0.46})O_3$ sample using the HRPD instrument.[24] Figure 4(a) shows the simulated NPD patterns for the space groups $R3m$ and $R3c$ and Fig. 4(b) shows the corresponding simulated x-ray powder diffraction patterns. Both figures were generated by the program POWDERCELL,[28] assuming a wavelength of 1.4700 Å. Figure 4(b) demon-

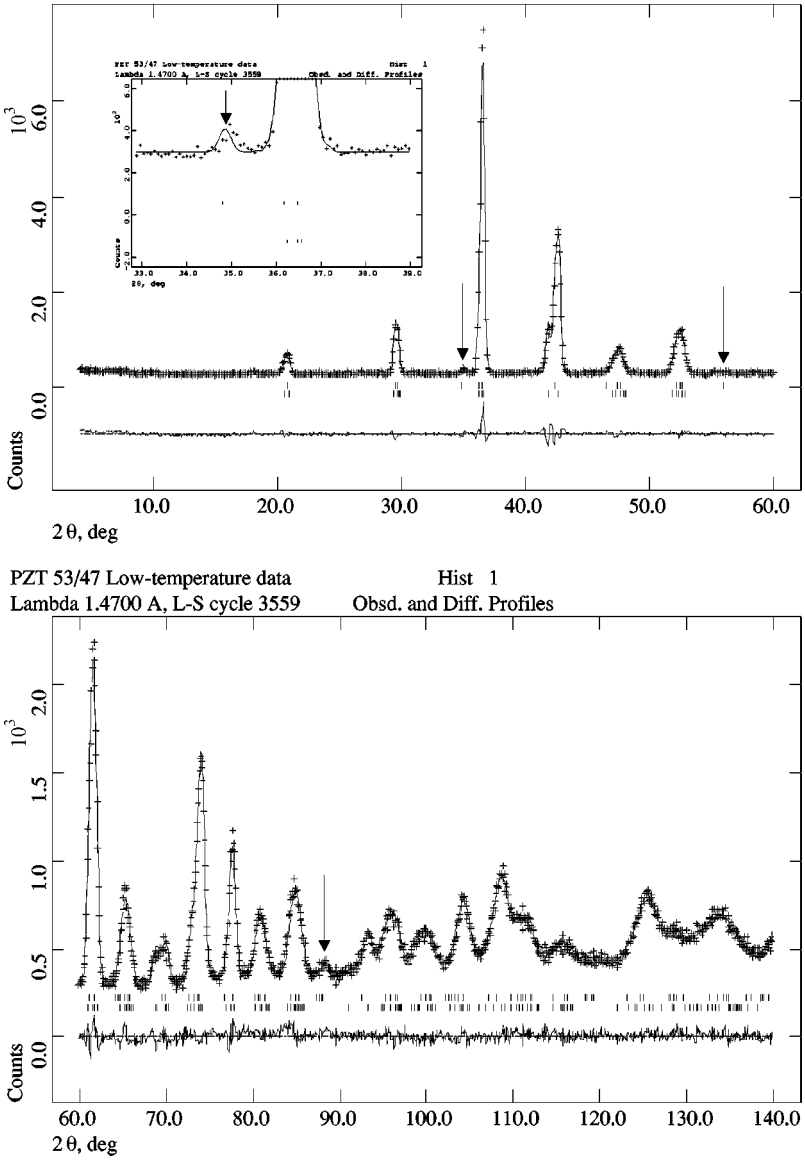

FIG. 3. Observed and calculated constant wavelength NPD (Studsvik) profile and its difference curves for a $Pb(Zr_{0.53}Ti_{0.47})O_3$ sample at 10 K. Top: small-2θ region. Bottom: large-2θ region. Peaks allowing the identification of the $R3c$ phase are indicated by arrows. Note the nonvanishing intensities of the peaks at around 35° (see inset), 56°, and 88°. The tick marks shown, from up to down, correspond to the Bragg reflections from the $R3c$ and Cm phases, respectively.

strates that it is practically impossible to distinguish the $R3m$ and $R3c$ phases by x rays, as the diffraction patterns are essentially identical. The reflections which are characteristic only for the $R3c$ phase have a vanishing intensity in the case of x rays. At compositions around the $x=0.50$ value even the observation of the presence of a rhombohedral phase by x-ray techniques is difficult, as the phase fraction of this phase is small for these compositions (see the $x=0.52$ data in Table I). This further points out that the nature of the phase transition is peculiar, obscured by the inhomogeneities always present in the samples. These inhomogeneities, most notably composition fluctuations, are able to create the ''two-phase coexistences'' PZT ceramics are so notorious for. In the case of x rays, this area (corresponding to $2\theta \approx 93.2°$, when the Cu K_α radiation is used) has very weak (practically nonobservable) Bragg reflections, and, contrary to the NPD data, this regime is not suitable for phase identification by x rays. In the case of x-ray diffraction, this type of two-phase coexistence is seen in ''anomalous'' line shapes.

C. Quantitative estimation of composition fluctuation

To make a quantitative estimation of the composition fluctuation and phase boundary location we assume that the composition distribution $cd(x)$ is temperature independent and is further describable by the Gaussian distribution $cd(x)=(\sqrt{2\pi}\sigma)^{-1}\exp[-(x-\mu)^2/(2\sigma^2)]$, where σ characterizes the composition fluctuation and μ is the average composition (for simplicity, taken here to be the nominal composition). If $\sigma \ll 1$, the phase fractions can be quickly estimated,

TABLE II. Fractional coordinates for the hexagonal setting of the space group $R3c$, as specified using the parameters s, t, d, and e, adapted from Refs. 25 and 26.

	x	y	z
Pb	0	0	$s+1/4$
Ti/Zr	0	0	t
O	$1/6-2e-2d$	$1/3-4d$	1/12

TABLE III. Parameters s, t, d, e, and ω, computed from the data given in Table I, are given, together with the parameters l and Δl (definitions for l and Δl are adapted from Ref. 29). Tilt angle ω is computed using the equation $\tan\omega = 4\sqrt{3}e$. Also the value of K is computed using the equation $a = 2Kl\cos\omega$; see Ref. 29.

x	0.52	0.53	0.53
T	10	295	10
s	0.034(5)	0.0294(24)	0.0336(24)
t	0.0023	0.0083	0.0114
d	−0.0052(8)	−0.0035(5)	−0.0037(5)
e	0.0147(22)	0.0035(23)	0.0127(14)
ω (deg)	5.81(86)	1.39(91)	5.03(55)
l (Å)	2.8867(43)	2.8761(41)	2.8810(26)
Δl (Å)	0.1797(43)	0.1213(41)	0.1275(26)
K	1.000	1.000	1.000

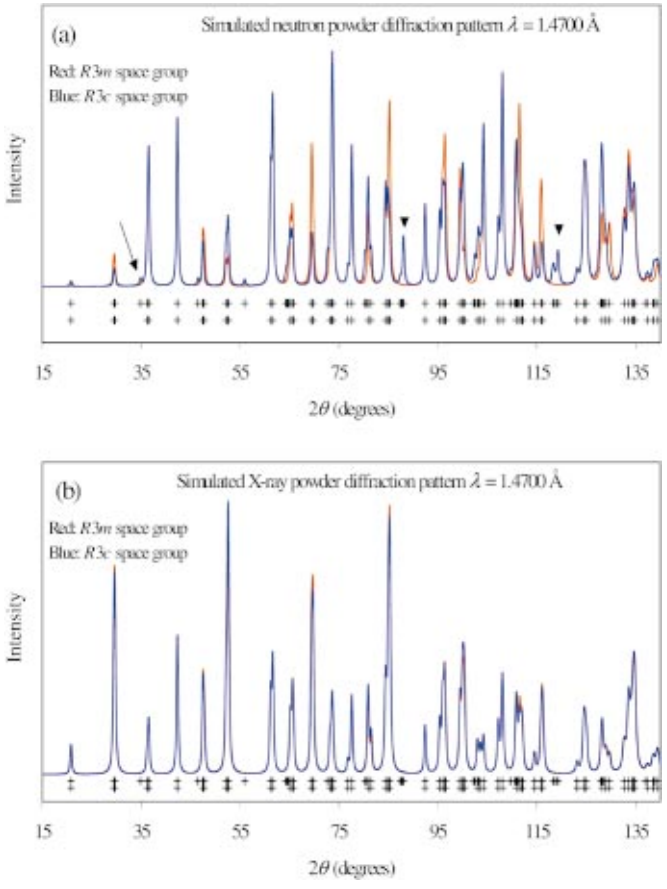

FIG. 4. (Color) Simulated powder diffraction patterns of the space groups $R3m$ and $R3c$ (a) in the case of neutrons and (b) in the case of x rays. In both cases the wavelength was 1.4700 Å, and the hexagonal lattice parameters were $a = 5.7400$ Å and $c = 7.0992$ Å (space group $R3m$) and $a = 5.7400$ Å and $c = 14.1985$ Å (space group $R3c$). The crosses shown, from top to bottom, correspond to the Bragg reflections from the $R3c$ and $R3m$ phases, respectively.

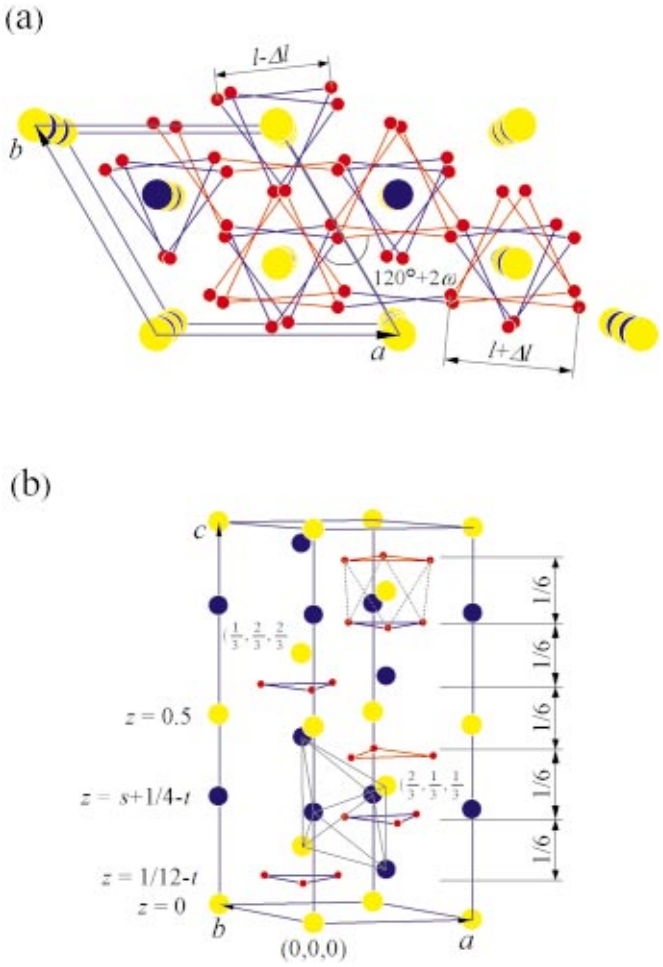

FIG. 5. (Color) Structural parameters of the low-temperature rhombohedral (space group $R3c$) PZT. (a) The plane perpendicular to the hexagonal c axis. Oxygen octahedral tilt angle ω and two equilateral oxygen triangle edge lengths $l-\Delta l$ (blue lines) and $l+\Delta l$ (red lines), as defined by Thomas and Beitollahi (Ref. 29) are shown. (b) Six equidistant oxygen layers in a hexagonal unit cell. Also the three lattice points and parameters s and t, defined in Table II, are shown. In both figures, oxygen ions are presented by red spheres and Pb and B cations by blue and yellow spheres, respectively. Oxygen octahedra surrounding the B cations and the octahedra formed by four Pb ions and two B cations surrounding the oxygen ion are shown.

for example, by using tables for the standard normal distribution function (see, e.g., Ref. 43). Labeling the location of the phase boundary by $x(T)$ the phase fraction of the rhombohedral phase is approximately $\int_{x(T)}^{\infty} cd(x)dx$. By substituting $z = (x-\mu)/\sigma$ we can take benefit from tables for the areas under the standard normal distribution from 0 to z. Taking the numerical values for phase fractions from the Table I and assuming that σ is the same for both samples we have the equations $1.14 = [x(10\,\mathrm{K}) - 0.52]/\sigma$ and $0.56 = [x(10\,\mathrm{K}) - 0.53]/\sigma$ which yield $\sigma = 1.7\%$ and $x(10\,\mathrm{K}) = 0.540$. In a similar manner we can estimate the phase boundary location at room temperature (recalling that σ and μ were assumed to be temperature independent) to be at $x = 0.538$. The inclination of the phase boundary is in an op-

posite direction to the one extrapolated from the phase diagram shown in Ref. 16, but this inclination is very small and thus it is not possible to judge if it is true phenomenon or just due to the various errors, e.g., in phase fraction estimation.

This type of estimation allows one to determine the location of the phase boundary as a function of temperature by collecting NPD data at different temperatures from two samples prepared through the same procedure but having slightly different but known average compositions. As the values obtained for the phase boundary and composition fluctuation are reasonable, they offer a neat explanation for the observed two-phase ''coexistence'' observed in the vicinity of the phase boundary. It also takes the temperature dependence into account.

V. POLYHEDRAL VOLUME RATIOS AND OCTAHEDRAL TILTING

As Thomas and Beitollahi[29] and Woodward[30,31] have previously discussed, the study of octahedral and cuboctahedral volumes gives essential information for the study of the stability of the crystal structure under consideration. It is particularly useful in the case of solid solutions, as it offers a way to predict or at least understand symmetry changes due to the atom substitutions, such as Zr for Ti. For a space groups corresponding to the tilt system $a^0a^0a^0$ (using Glazer notation[32]) the volume ratio between the cuboctahedral volume V_A and octahedral volume V_B is $\underline{5}$ (see, e.g., Ref. 29). This is the case of space groups $Pm\bar{3}m$, $P4mm$, $Pmm2$, $Cmm2$, Pm, Cm, and $R3m$. However, in the case of the space group $R3c$ the octahedral tilt system ($a^-a^-a^-$) allows this ratio to be below 5. The relationship between the tilt angle ω defined by Megaw and Darlington[25] and the ratio V_A/V_B is given by the equation $V_A/V_B=6K^2\cos^2\omega-1$, where $K\approx1$ (see the more detailed discussion in Ref. 29). This value, together with the short and long oxygen distances $l-\Delta l$ and $l+\Delta l$, respectively, is tabulated in Table III (see also Ref. 33). *The V_A/V_B ratio of the $R3c$ phase decreases with decreasing temperature: crystal is contracting with decreasing temperature and thus the B cations (which fit oxygen octahedra tightly) have to take larger relative volume from the total volume (from the cuboctahedra, which has "excess" of space for Pb) by tilting oxygen octahedra*. Figures 5(a) and 5(b) illustrate the rhombohedral unit cell and these two parameter sets.

It is also interesting to note the behavior of the volume per formula unit, Ω, as a function of composition and temperature, shown in Table IV. Two things can be observed immediately: for $x=0.50$ the phase which gave better statistical figures of merit at 10 K (space group Cm, in contrast to the $P4mm$ symmetry) also had a larger Ω value. At 295 K it was difficult to judge from the diffraction data whether the space group should be assigned to $P4mm$ or Cm (or even to an orthorhombic phase), as is also reflected by the fact that the volumes corresponding to these two symmetries are essentially identical. As a second point, at 10 K the $R3c$ phase ($x=0.52$ and $x=0.53$ samples) had larger Ω values than the Cm phase. For example, in the case of the $x=0.53$ sample, the volume per formula unit of the $R3c$ phase was larger than in the case of the Cm phase, at 10 K and at 295 K. In principle, these observations can be understood from the point of view of the *maximum volume principle*. In PZT ceramics, bonding is dominated by interionic electrostatic forces, and the repulsion of next-nearest-neighbor ions of the same charge favors a volume expansion, as was discussed in Refs. 34 and 35. Thus, the symmetry with larger Ω value might correspond to the stable phase, but this is difficult to judge. Although the equation given in Fig. 1 is rather crude for the study of the delicate balance between the competing phases at the vicinity of MPB (as it fits nearly the whole composition region, which is rather rough approximation once one considers the fact that there might be abrupt changes in volume once the symmetry is changed, for example, from $P4mm$ to $R3c$), it gives some idea about the change of Ω against composition fluctuations. Namely, once x changes by an amount of 0.01, Ω changes by an amount of 0.0875 Å^3, which is the same order of magnitude as the typical standard errors of Ω; see Table IV.

TABLE IV. Volume per formula unit, Ω, computed for three compositions at two temperatures. Lattice parameters for $x=0.50$ sample are from Ref. 15. Also the cuboctahedral volume V_A and octahedral volume V_B are given.

x	Space group	T (K)	Ω (Å^3)	V_A	V_B	V_A/V_B
0.50	$P4mm$	295	67.325(4)	56.104	11.221	5
0.50	Cm	295	67.324(6)	56.104	11.221	5
0.50	$P4mm$	10	67.176(5)	55.980	11.196	5
0.50	Cm	10	67.183(7)	55.986	11.197	5
0.52	Cm	295	67.47(3)	56.221	11.244	5
0.52	$P4mm$	295	67.60(33)	56.336	11.267	5
0.52	Cm	10	67.294(12)	56.078	11.216	5
0.52	$R3c$	10	67.68(5)	56.283	11.397	4.9382
0.53	Cm	295	67.54(3)	56.282	11.256	5
0.53	$R3c$	295	67.75(2)	56.452	11.298	4.9965
0.53	Cm	10	67.32(17)	55.100	11.220	5
0.53	$R3c$	10	67.52(2)	55.182	11.340	4.9542

Is the monoclinic phase stable?

It is clear from the various studies[1–4,6,15,21] that the Cm phase exists in a composition range $0.50\lesssim x\lesssim0.54$ at and below room temperature (in Refs. 2 and 3 the nearly temperature-independent phase boundary between the Cm and rhombohedral phases was assigned to be at $x\approx0.54$, consistently with the value determined in Sec. IV C). It is, however, important to note that it typically coexists with another phase, either with a $P4mm$ (Ti-rich compositions) or rhombohedral (either $R3m$ or $R3c$) phase (Zr-rich compositions), due to the composition fluctuation. Note that this is also the case for the *low-temperature* structure reported by Noheda *et al.*,[3] as they do mention that at 20 K their NPD pattern from a $Pb(Zr_{0.52}Ti_{0.48})O_3$ sample did show a weak superlattice reflection not explainable by the Cm symmetry. The simplest explanation is that they do have the $R3c$ phase as a secondary phase. However, the phase fraction of this

phase is rather low for this composition (at 10 K, 13 wt % in our case; see Table I) and, as discussed above, is not easily seen by x rays they typically use in their studies. Further, even NPD data reveal the $R3c$ phase most clearly at low temperatures, where the octahedral tilt differs sufficiently from zero. The phase structure of the $x=0.52$ sample at room temperature is not clear, as the intensity between the $(h00)$ and $(00l)$ reflections (using cubic indexing) is not solely explainable by the Cm phase. For $x=0.52$ sample at 295 K we used $P4mm$ symmetry to model this contribution, as there were two phases also at 10 K. However, we could not unambiguously assign a space group symmetry for this phase or even exclude the contribution of diffuse scattering to this intensity.

Cm symmetry allows a relieving of stress, which would otherwise be generated due to the interacting rhombohedral and $P4mm$ phases.[36] Also this explanation is based on assumption that there is composition fluctuation, as it is probably the underlying reason for the two-phase coexistence. The line broadening of the Cm phase was dependent on temperature and reflection indices hkl, which is probably due to the microstrain effects.[24] Further, it is interesting to note that the volume per primitive cell, Ω, of the $R3c$ phase is larger than that of the Cm phase for $x=0.52$ and $x=0.53$ samples; see Table IV. This hints that at and below room temperature near the MPB the $R3c$ (above-room-temperature $R3m$) phase might be the true stable phase for $x \gtrsim 0.53$ and the $P4mm$ phase might be the stable one for lower x values. However, conclusions based on volume estimations are strictly valid only if there is no composition fluctuation. A more reliable idea about the phase stabilities against composition and temperature is obtained via weight fractions, see Table I.

VI. SPONTANEOUS POLARIZATION

We estimated spontaneous polarization $\mathbf{P}_s$ for $P4mm$, Cm, and $R3c$ phases by the dipole moment equation $\mathbf{P}_s \approx (1/V)\Sigma_i q_i \mathbf{r}_i$, where the sum is over the point charges q_i at positions $\mathbf{r}_i$ in a primitive cell volume V. This is an approximation with its limitations, as is discussed below.

A. Tetragonal PZT ceramics

Assuming that Pb ions are located at the origin (which is a simplification), B cations at the positions $(1/2,1/2,1/2+\delta(B))$ [allowing the z coordinates of Zr and Ti ions to be different; i.e., $\delta(B)$ is either $\delta(\mathrm{Zr})$ or $\delta(\mathrm{Ti})$], oxygen ions O_1 at the positions $(1/2,1/2,\delta(O_1))$ and oxygen ions $O_{2,3}$ at the positions $(1/2,0,1/2+\delta(O_{2,3}))$ and $(0,1/2,1/2+\delta(O_{2,3}))$. The direction of $\mathbf{P}_s$ coincides with the c-axis direction and can be estimated by the equations

$$\mathbf{P}_s = e\{4[x\,\delta(\mathrm{Zr})+(1-x)\,\delta(\mathrm{Ti})]-4\,\delta(O_{2,3})-2\,\delta(O_1)\}\hat{\mathbf{z}}/a^2 \tag{1}$$

$$\approx e\{4[x\,\delta(\mathrm{Zr})+(1-x)\,\delta(\mathrm{Ti})]-6\,\delta(O)\}\hat{\mathbf{z}}/a^2, \tag{2}$$

where a and c are the lattice parameters, $\hat{\mathbf{z}}$ is the unit vector along the c-axis direction, and e is the elementary charge.

B. Monoclinic PZT ceramics

We assume that Pb ions are located at the origin, B cations at the positions $(1/2-\delta_x(B),0,1/2+\delta_z(B))$, oxygen ions O_1 at the positions $(1/2+\delta_x(O_1),0,\delta_z(O_1))$, and oxygen ions $O_{2,3}$ at the positions $(1/4+\delta_x(O_{2,3}),1/4+\delta_y(O_{2,3}),1/2+\delta_z(O_{2,3}))$ and $(1/4+\delta_x(O_{2,3}),-1/4-\delta_y(O_{2,3}),1/2+\delta_z(O_{2,3}))$. Now, $\mathbf{P}_s$ is constrained by symmetry to the ac plane, and thus it has two components

$$\mathbf{P}_s = \mathbf{P}_{s,x} + \mathbf{P}_{s,z}, \tag{3a}$$

$$\mathbf{P}_{s,x} = 2e\{4[x\,\delta_x(\mathrm{Zr})+(1-x)\,\delta_x(\mathrm{Ti})]-4\,\delta_x(O_{2,3}) - 2\,\delta_x(O_1)\}\hat{\mathbf{x}}/(ac\sin\beta), \tag{3b}$$

$$\mathbf{P}_{s,z} = 2e\{4[x\,\delta_z(\mathrm{Zr})+(1-x)\,\delta_z(\mathrm{Ti})]-4\,\delta_z(O_{2,3}) - 2\,\delta_z(O_1)\}\hat{\mathbf{z}}/(ab\sin\beta), \tag{3c}$$

$$\theta = \overline{\arccos}[P_{s,z}\sin\beta/\sqrt{(P_{s,x}+P_{s,z}\cos\beta)^2+(P_{s,z}\sin\beta)^2}], \tag{3d}$$

where θ is the angle between the pseudocubic c axis (more precisely, the direction perpendicular to the monoclinic a and b axes) and $\mathbf{P}_s$.

C. Rhombohedral PZT ceramics

In PZT ceramics with $R3c$ symmetry, ions are at the positions given in Table II. Now, $\mathbf{P}_s$ is along the hexagonal c axis,

$$\mathbf{P}_s = \frac{24e}{\sqrt{3}a^2}(2t+s)\hat{\mathbf{z}}, \tag{4}$$

where s and t are defined in Table II, and e is the elementary charge.

D. Polarization behavior as a function of x and temperature

Equations (2), (3), and (4) are approximations based on the assumption of point charges (ions with their nominal charges). Further, they do not take into account the domain contribution or the electronic polarizability, which both have an influence on the experimentally determined value for $\mathbf{P}_s$ [see also an interesting first-principles study of piezoelectricity in $Pb(Zr_{0.50}Ti_{0.50})O_3$ in Ref. 37, as it discusses the important role of the electronic part of the polarization ignored in our qualitative discussion]. Once taking into account that in practice the electron distribution of the B cations is concentrated near the adjacent oxygen plane (such as the $O_{2,3}$ plane perpendicular to the c axis of the $P4mm$ phase), this value can be considered as an upper limit of the $\mathbf{P}_s$. Table V tabulates the estimations for P_s, as computed from Eqs. (2), (3), and (4) and experimental ion positions given in Tables I and VI. It is seen that the polarization decreases with increasing x and temperature. It is also interesting to note that the direction of $\mathbf{P}_s$ in Cm phase approaches the pseudocubic $\langle 111\rangle$ direction as x increases and temperature decreases, in accordance with the phase transition to the rhombohedral phase; see Table V.

TABLE V. Spontaneous polarization for various PZT compositions. In PZT ceramics with the $P4mm$ symmetry, the polarization direction is along the c axis, in the case of the Cm symmetry it is in a plane determined by the monoclinic a_M and c_M axes, and in the case of the $R3c$ phase it is along the hexagonal c axis. In the case of Cm symmetry, we also give the direction angle θ [see Eq. (3d)] and compare it to the "rhombohedral direction angle" $\theta_R \approx \overline{\arccos}(c_M/\sqrt{a_M^2+c_M^2})$.

x	0.20	0.30	0.40	0.50	0.52	0.52	0.53	0.53	0.53	0.53
T (K)	295	295	295	295	10	10	295	295	10	10
Space group	$P4mm$	$P4mm$	$P4mm$	$P4mm$	Cm	$R3c$	Cm	$R3c$	Cm	$R3c$
P_s (μC cm^{-2})	48.9	47.0	41.7	36.4	39.7	26.2	37.3	31.0	37.9	38.1
$P_{s,x}$ (μC cm^{-2})					7.5		−1.5		11.4	
$P_{s,z}$ (μC cm^{-2})					39.0		37.3		36.2	
θ (deg)					10.5		2.6		17.0	
θ_R (deg)					54.1		54.2		54.3	

VII. BOND-VALENCE CALCULATIONS

Bond-valence calculations were carried out to estimate the reliability of the structural models. Particularly, the observations related to the different positions of Zr and Ti ions can be estimated via these computations. In the BVC model (see Ref. 38 and Refs. 34 and 39; note that these two more recent references give a more general set of parameters), the electrostatic bond strength is given by the empirical relationship $s_{ij}=\exp B(R_{ij}-d_{ij})$, where s_{ij} is the bond valence between atoms i and j, R_{ij} is a constant specific to that pair of atoms, B is a constant equal to 1/0.37, and d_{ij} is the bond length, in angstroms. Room-temperature values of R_{ij} (labeled as R_{ij}^{RT}) for atom pairs Pb-O, Zr-O, and Ti-O are 2.097 88, 1.951 46, and 1.814 38, respectively.[34,39] However, R_{ij} parameters are dependent on temperature. The method of correction for temperature is given in Refs. 40 and 41. Following this procedure we determined the corresponding parameters at 10 K, $R_{\mathrm{Pb\text{-}O}}^{10\ \mathrm{K}}$, $R_{\mathrm{Zr\text{-}O}}^{10\ \mathrm{K}}$, and $R_{\mathrm{Ti\text{-}O}}^{10\ \mathrm{K}}$, by using the approximations $R_{\mathrm{Pb\text{-}O}}^{10\ \mathrm{K}} \approx R_{\mathrm{Pb\text{-}O}}^{\mathrm{RT}} + \frac{1}{12}\sum_{i=1}^{12}[d_{(\mathrm{Pb\text{-}O})i}^{10\ \mathrm{K}} - d_{(\mathrm{Pb\text{-}O})i}^{295\ \mathrm{K}}]$, $R_{\mathrm{Zr\text{-}O}}^{10\ \mathrm{K}} \approx R_{\mathrm{Zr\text{-}O}}^{\mathrm{RT}} + \frac{1}{6}\sum_{i=1}^{6}[d_{(\mathrm{Zr\text{-}O})i}^{10\ \mathrm{K}} - d_{(\mathrm{Zr\text{-}O})i}^{295\ \mathrm{K}}]$, and $R_{\mathrm{Ti\text{-}O}}^{10\ \mathrm{K}} \approx R_{\mathrm{Ti\text{-}O}}^{\mathrm{RT}} + \frac{1}{6}\sum_{i=1}^{6}[d_{(\mathrm{Ti\text{-}O})i}^{10\ \mathrm{K}} - d_{(\mathrm{Ti\text{-}O})i}^{295\ \mathrm{K}}]$; i.e., for each $R_{ij}^{10\ \mathrm{K}}$ we averaged over all the bonds around a given cation (12 bonds for Pb and 6 for both Zr and Ti). Further, corrections were separately carried out for the $R3c$ and Cm phases. At 10 K, we used the same correction for the $x=0.52$ and $x=0.53$ samples in the case of the $R3c$ phase (obtained from the $x=0.53$ data). Correction for temperature (in this temperature range) changed the valence values approximately by 1%.

Tables I and VI give the experimentally observed structural parameters used in this BVC study (from. Refs. 6 and 21); see also Ref. 42. Table VII lists the valences of Pb, Zr,

TABLE VI. Structural parameters for the PZT ceramics used in this study, in addition to those listed in Table I. NPD data for tetragonal structures were adapted from Ref. 6 and for monoclinic structures from Ref. 21. In the case of monoclinic structure, $y(\mathrm{Zr,Ti})=y(\mathrm{O}_1)=0$. Data were refined using Rietveld refinement.

x	0.20	0.30	0.40	0.50	0.52
Space group	$P4mm$	$P4mm$	$P4mm$	$P4mm$	Cm
T (K)	295	295	295	295	295
a (Å)	3.952 515(25)	3.978 025(23)	4.004 298(25)	4.030 341(34)	5.7082(20)
b (Å)					5.7078(18)
c (Å)	4.148 40(6)	4.148 77(5)	4.149 64(5)	4.144 90(7)	4.141 44(33)
β (deg)					90.199(16)
x(Pb)	0.0085(12)	0.0146(7)	0.0230(5)	0.0240(5)	0
$=y$(Pb)					
z(Pb)	0.0000(19)	0.0000(26)	0.000(6)	0.0000(7)	0
x(Zr)					0.500(9)
z(Zr)	0.5632(21)	0.5604(9)	0.5641(19)	0.5649	0.572(4)
x(Ti)					0.517(19)
z(Ti)	0.5452	0.5468	0.5580	0.5649	0.594(13)
$x(\mathrm{O}_1)$					0.4751(22)
$z(\mathrm{O}_1)$	0.1035(19)	0.1011(26)	0.0997(6)	0.0921(7)	0.0872(16)
$x(\mathrm{O}_{2,3})$					0.2328(24)
$y(\mathrm{O}_{2,3})$					0.2466(12)
$z(\mathrm{O}_{2,3})$	0.6162(19)	0.6165(26)	0.615(6)	0.6110(7)	0.6071(13)

TABLE VII. Cation valences estimated by applying bond-valence method to NPD data (from Refs. 6, 15, and 21, and Table VI). For Pb ions in tetragonal structure, two values are given. The left-hand one indicates the valence when Pb ion was fixed to origin, and the right-hand one takes into consideration that Pb ions were shifted into the ⟨110⟩ direction (Ref. 6). Also an average valence for the *B* cations is given, $v(B_{av})=xv(\mathrm{Zr})+(1-x)v(\mathrm{Ti})$. Oxygen valencies were also computed. The length of the line between oxygen and cation (Zr or Ti) indicates the bond lengths, which are different with the exception of the $P4mm$ symmetry and $O_{2,3}$ ion.

x	0.20	0.30	0.40	0.50	0.52	0.52	0.52	0.53	0.53	0.53	0.53
Space group	$P4mm$	$P4mm$	$P4mm$	$P4mm$	Cm	Cm	$R3c$	Cm	$R3c$	Cm	$R3c$
T (K)	295	295	295	295	295	10	10	295	295	10	10
v(Pb)	1.96, 1.97	1.90,1.92	1.83,1.86	1.76,1.79	1.85	2.08	2.02	1.86	1.77	1.94	1.95
v(Zr)	5.20	5.07	4.93	4.80	4.77	4.78	4.81	4.82	4.68	4.74	4.70
v(Ti)	3.64	3.54	3.42	3.31	3.36	3.30	3.32	3.33	3.23	3.27	3.25
$v(B_{av})$	3.95	4.00	4.02	4.05	4.09	4.07	4.11	4.10	4.00	4.03	4.02
Zr–O—Zr $v(O_1)$, $v(O_{2,3})$	2.14,2.51	2.12,2.43	2.06,2.35	2.00,2.28	2.05,2.29	2.25,2.31	2.28	2.18,2.25	2.15	2.24,2.22	2.22
Zr–O—Ti $v(O_1)$, $v(O_{2,3})$	1.96,2.22	1.90,2.15	1.78,2.09	1.70,2.02	1.90,1.99	2.08,2.05	2.08	2.02,2.05	1.90	2.07,1.98	1.95
Ti–O—Zr $v(O_1)$, $v(O_{2,3})$	1.94,2.22	1.93,2.15	1.89,2.09	1.83,2.02	1.72,2.12	1.65,2.06	1.98	1.85,1.95	1.92	1.93,1.96	2.00
Ti–O—Ti $v(O_1)$, $v(O_{2,3})$	1.76,1.92	1.71,1.86	1.61,1.82	1.53,1.77	1.57,1.83	1.78,1.80	1.78	1.69,1.75	1.67	1.76,1.72	1.73
$v(O_{1av})$	1.84	1.83	1.79	1.77	1.82	1.95		1.95		2.02	
$v(O_{2,3av})$	2.04	2.03	2.03	2.02	2.07	2.07		2.01		1.98	
$v(O_{av})=\frac{1}{3}v(O_1)+\frac{2}{3}v(O_{2,3})$	1.97	1.97	1.95	1.94	1.99	2.03	2.04	1.99	1.93	1.99	1.99
$\Sigma_i v_i$	0.00	−0.01	0.00	−0.01	−0.03	0.06	0.01	−0.07	−0.02	0.00	0.00

and Ti ions and the average valences of Zr and Ti [labeled as v(Pb), v(Zr), v(Ti), and $v(B_{av})$, respectively], for several PZT compositions. It is seen that v(Zr) is anomalously large and v(Ti) is rather low. This is plausible, as the average unit cell size is ''too small'' for Zr ions, which makes the bonds abnormally short. The contrary is true for Ti ions. Similar values were found in Ref. 29 for rhombohedral PZT ceramics. However, as the volume per formula unit increases with increasing x, v(Zr) decreases (mainly due to the increased Zr-O_2, O_3 bond lengths). To have a more affirmative base, oxygen valencies were also computed. This was slightly trickier than the computation of cation valencies. In the case of $P4mm$ and Cm symmetries, there are two nonequivalent oxygens O_1 and O_2, and in a case of $R3c$ symmetry there is only one oxygen in an asymmetric unit. In each case, each oxygen is surrounded by ''cation octahedra'' formed from four Pb and two *B* cations, as is indicated in Fig. 5 in the case of $R3c$ symmetry. As there is no evidence for *B* cation ordering, we assumed that Zr and Ti ions are randomly distributed over the *B* cation sites. Thus, the probability that the *B* site is occupied by Zr is x, and correspondingly the probability that it is occupied by Ti is $1-x$. In general, we have to consider four kind of possibilities: namely, that the vertices of cation octahedra are both occupied by Zr or by Ti or that one vertice is occupied by Ti and the other by Zr. These last two cases lead to different oxygen valencies in all cases but the $P4mm$ symmetry and O_2 ion. Table VII indicates these cases for each oxygen and also gives average values. These average values were computed assuming that the cation octahedra vertice occupation probabilities for different cases are as follows: case Zr,Zr: x^2, case Ti,Ti: $(1-x)^2$, case Zr,Ti: $x(1-x)$, and case Ti,Zr: $(1-x)x$.

The position of Zr ions is approximately constant as a function of Zr content for $x \leqslant 0.52$. The shift along the c axis would lead to an increase in v(Zr) and $v(B_{av})$, preventing the motion of Zr. The shift of Ti ions closer to the oxygen O_2, O_3 plane perpendicular to the c axis partially compensates the valence loss due to the lengthened Ti-O_2, O_3 bonds. For tetragonal compositions, the valence of Pb ions was lower than the nominal valence +2 and decreased with increasing x, until it slightly increased at $x=0.52$, corresponding to the change to Cm symmetry. Thus, in the $P4mm$ phase, the rather strong decrease of v(Pb) with increasing x was mainly compensated for by the increasing $v(B_{av})$ and, to a lesser extent, by decreasing $v(O_{av})$. The region at around $x=0.52$ is of particular interest, as it is the well-known area of two-phase coexistence. By considering the valence behavior of the competing phases one gains insight into the reasons of phase transitions. This region also shows that v(Pb) increases and the *B* cation valences remain nearly constant with decreasing temperature. This is well demonstrated by the behavior of the $x=0.53$ sample in Table VII and is easily understood by considering the fact that due to the increased octahedral tilt, the volume of cuboctahedra is decreased [which decreases Pb-O bond lengths and thus increases v(Pb)] and the volume of octahedra is increased, so that it is indeed larger at 10 K than at 295 K [due to the increased Zr/Ti-O bond lengths, v(Ti) and v(Zr) decrease].

A. Fractional coordinates of Zr and Ti ions

We also determined ''optimal positions'' for Zr and Ti ions for tetragonal PZT ceramics at room temperature (i.e., we fitted the fractional z coordinate of Zr and Ti ions to the experimentally observed lattice and oxygen parameters at room temperature), and list them in Table VIII. It is seen that there is no position in a tetragonal unit cell, where v(Zr) would be +4, although two such kind of positions can be found for Ti, as is indicated in the second column of Table VIII. Neither of the two minima for Ti ion are physically

TABLE VIII. Fractional z coordinates of Zr and Ti ions corresponding to the minimum valence of Zr ion, $z(\mathrm{Zr},v(\mathrm{Zr})_{min})$, positions of Ti where $v(\mathrm{Ti})=+4$, $z(\mathrm{Ti},v(\mathrm{Ti})=+4)$, and positions of Ti, when $v(B_{av})=+4$ and $v(\mathrm{Zr})=v(\mathrm{Zr})_{min}$, labeled as $z(\mathrm{Ti},v(B_{av})=+4)$. The values in bold are most consistent with the experimental results.

x	$z(\mathrm{Zr},v(\mathrm{Zr})_{min})$, $v(\mathrm{Zr})_{min}$	$z(\mathrm{Ti},v(\mathrm{Ti})=+4)$, $v(B_{av}),v(\mathrm{Ti})=+4)$	$z(\mathrm{Ti},v(B_{av})=+4)$, $v(\mathrm{Ti})$	$z(\mathrm{Ti})=z(\mathrm{Zr})$, $v(B_{av})=+4$
0.20	**0.592**, 5.16	0.495, 0.699, 4.23	**0.531**, 0.657, 3.71	0.539, 0.648
0.30	**0.588**, 5.03	0.485, 0.703, 4.31	**0.541**, 0.638, 3.56	0.551, 0.627
0.40	**0.587**, 4.90	0.479, 0.709, 4.36	**0.570**, 0.606, 3.40	0.575, 0.601
0.50	**0.578**, 4.79	0.466, 0.705, 4.40	**0.578**, –, 3.30 [a]	0.578, – [a]

[a]The minimum $v(B_{av})$ value was 4.04.

meaningful, as they correspond to $r_{\mathrm{Ti}}+r_{\mathrm{O}}$ values between 1.60 and 1.63 Å, far too small to be reliable ($r_{\mathrm{Ti}}=0.61$ Å and $r_{\mathrm{O}}=1.40$ Å, see, e.g., Ref. 43). Also the second minima, given in the third column, are rather high, especially at low Zr values, and are questionable (also corresponding to small $r_{\mathrm{Ti}}+r_{\mathrm{O}}$ values). Thus, we concentrate on the values indicated by bold font in Table VIII. Interesting features of these results are that the position of Zr was always closer to the center of the oxygen O_2, O_3 plane perpendicular to the c axis than Ti ions, i.e., that $z(\mathrm{Zr},v(\mathrm{Zr})_{min})>z(\mathrm{Ti},v(B_{av})=+4)$ and that $z(\mathrm{Ti},v(B_{av})=+4)$ is increasing with increasing x. This increase was 0.047, and the corresponding decrease of $z(\mathrm{Zr},v(\mathrm{Zr})_{min})$ was 0.014, when x increased from 0.20 to 0.50. This is well consistent with the experimental results (compare the values typed by bold font in Tables VI and VIII). Thus, for tetragonal compositions the structure can maintain the average B cation valence of +4 by shifting the Zr ion into a position where $v(\mathrm{Zr})$ has the minimum value $v(\mathrm{Zr})_{min}$ and adjusting the position of Ti so that $v(B_{av})=+4$. It means that the oxygen octahedral network and partially the valence-deficient Pb maintain the equality $v(B_{av})=+4$ (and, due to the charge neutrality, the overall valence of cations and anions should be zero). As the amount of Zr ions is increasing (the limit being at around $x=0.50$), there is no such positions for Zr and Ti ions that $v(B_{av})$ would be +4. However, when the Zr ions are shifted into $\langle hhl\rangle$ or $\langle 111\rangle$ directions (Cm and $R3c$ symmetries, respectively), it becomes possible to decrease $v(\mathrm{Zr})$ and $v(B_{av})$. It is possible to constrain Ti and Zr ions to have the same coordinates and $v(B_{av})$ to be +4 [except for the $x=0.50$ sample, where the minimum value of $v(B_{av})$ was 4.04 and which, interestingly, corresponded to the absolute minimum of $v(B_{av})$; i.e., it was not possible to find a lower value for $v(B_{av})$ by allowing the Ti and Zr ions to have different z coordinates]. It is also interesting to note that for $x=0.50$, the three values, $z(\mathrm{Zr},v(\mathrm{Zr})_{min})$, $z(\mathrm{Ti},v(B_{av})=+4)$, and $z(\mathrm{Ti})=z(\mathrm{Zr})$ coincide, exactly as was experimentally observed. However, for lower values of x this constraint was predicting two z-coordinate values (last column in Table VIII), the second one being rather questionable. Further, Rietveld refinements using this type of constraint were leading to meaningless z-coordinate and negative thermal parameters.[6]

We conclude that $v(B_{av})$ and $v(\mathrm{Pb})$ were close to the values +4 and +2, respectively, when $x<0.50$. As it was not anymore possible to fulfill these constraints for higher values of x *and tetragonal symmetry*, a phase transition to the Cm and $R3c$ symmetries occurs, allowing the values of $v(B_{av})$ and $v(\mathrm{Pb})$ to be +4 and +2, respectively. This is consistent with the observation that, namely, the symmetry Cm is experimentally observed, instead of the symmetry Pm. It might well be that also geometrically plausible $\langle hhl\rangle$-type displacements of the Zr ions force the displacements of the Pb ions to occur in the $\langle 110\rangle$ directions (and not in the $\langle 100\rangle$ directions). Thus, among the different symmetries the one fulfilling the constraints set by the nominal average valences is the one experimentally observed. Further, the oxygen octahedra tilt ($R3c$ symmetry) is understandable from this point of view. If there were no tilt, the oxygen octahedra volume would be $\Omega/6$ (corresponding to the $R3m$ phase), and this would again lead to too high values of $v(B_{av})$ at high Zr concentrations and/or at low-temperatures.

VIII. CONNECTION BETWEEN THE STRUCTURAL AND ELECTRICAL PROPERTIES

A. Role of Pb

To understand the factors behind the high susceptibility and piezoelectric coefficients of PZT ceramics, it is useful to borrow ideas from order-disorder ferroelectrics. Namely, we can roughly think that the structure of PZT ceramics consists of a rigid oxygen octahedral network, with Pb ions at the cuboctahedral sites. As x increases, the space for Pb ions increases, and as the NPD results indicate, Pb ions are moved significantly away from the cuboctahedral site center. This is common feature for the Pb containing perovskites; see, e.g., Ref. 44. As the cuboctahedral and octahedral volumes increase with increasing x and when this is combined with the fact that Pb^{2+} ions have a lone electron pair, larger shifts are possible. Now, we can think that the cuboctahedra include several potential energy minima for Pb ions. As the $x\approx 0.50$ composition is approached, the motion of Pb ions between different potential minima becomes significant. This is observed by Raman spectroscopy in the case of the $A_1(1\mathrm{TO})$ mode; see, e.g., Refs. 5 and 15. However, the Raman results discussed above demonstrate that the multiwell structure is not limited to the pseudocubic [001] direction, but there are also minima in a pseudocubic $\langle 110\rangle$ directions, analogously as Comes *et al.*[45] previously proposed their order-disorder model, in which there are eight sites along $\langle 111\rangle$ directions for low-energy distortions. Now, the minima

for Pb ions are shallow as one approaches the $x \approx 0.50$ composition, and correspondingly Pb ions can easily respond to the external electric field or pressure, which is crucial for the high susceptibility and piezoelectric coefficient.

B. Role of the *B* cations and oxygen octahedra

The contribution of the BO_6 unit in a response to the external field is twofold. In what follows, we shortly discuss the case where cation shifts are in a polarization direction. First, oxygen octahedra can move with respect to the Pb cage. Second, the *B* cations may move with respect to octahedra (which, in the case of larger shifts and tetragonal structure, necessitates that the *B* cations go through the oxygen $O_{2,3}$ plane perpendicular to the *c* axis, which obviously is more difficult the shorter the *a* axis is and the larger the *B* cation is). Similarly, as increasing the Zr concentration *x* increases the volume for Pb ions (volume of cuboctahedra), it increases the volume for the *B* cations. As is plausible from geometrical considerations, the response of Zr in a tetragonal structure to an external field is to move rigidly with the oxygen octahedra (and via the electronic part of the polarization). This is seen as a lower susceptibility. In contrast, smaller Ti ion cores are allowed to move easier between the potential energy minima. In tetragonal compositions, namely, Ti ion cores, in contrast to Zr ion cores, can respond to the external electric field (dielectric susceptibility), stress (piezoelectricity), and temperature (pyroelectricity). Further, as *x* increases, the susceptibility increases. This is due to the fact that Zr ions stretch the *a* axis and create space for Ti ions so that they can easily respond to the external fields. This model is valid as long as we consider quasistatic phenomena, i.e., in the cases where ions can follow the field.

The situation is changed once we approach the MPB. The octahedral volume is already sufficiently large to allow Zr to move with respect to the oxygen octahedra. On the other hand, if we consider the case of rhombohedral PZT and electric field applied along the hexagonal $\langle 001 \rangle$ direction, we can see that both *B* cations should be able to move with ease with respect to the oxygen octahedra. This is due to the fact that now the *B* cations are moving against the oxygen triangles (see Fig. 5), i.e., it is not necessary for the *B* cation to go through the oxygen plane in order to change the dipole moment direction created by oxygen octahedra and the *B* cation.

IX. CONCLUSIONS

Problems related to the determination of the structure of PZT ceramics were discussed from the neutron and x-ray powder diffraction (average symmetry) and Raman spectroscopy (local symmetry) points of view. Rietveld refinements carried out for the neutron powder diffraction data collected from $x = 0.52$ and $x = 0.53$ samples at 10 K showed that they consisted of coexisting Cm and $R3c$ phases. The room-temperature structure of the $x = 0.52$ sample was previously modeled by the Cm and $P4mm$ phases. The room-temperature structure of the $x = 0.53$ sample was modeled by the Cm and $R3c$ phases. The octahedral tilt angle of the $R3c$ phase was close to zero at room temperature (the zero tilt angle corresponds to the $R3m$ phase).

Bond-valence calculations were used to estimate the previously reported neutron powder diffraction data and to have a quantitative picture about the cation shifts with respect to the oxygen network. Agreement between the experimental results and these calculations was very good. We studied the cases where Zr and Ti ions were allowed to have different *z* coordinates, as was experimentally found to be true. It was found that the valence of Pb was slightly below $+2$ and that the valences of Zr and Ti were above and below $+4$, respectively. The oxygen valence was nearly -2. The composition-averaged *B* cation valence was found to be close to $+4$. For tetragonal compositions, the average *B* cation valence was increasing with increasing *x* and was accompanied by decreasing Pb cation valence. It was pointed out that the Zr and Ti ions adjust their positions so that the average valence is kept at a fixed value of $+4$. This was no more possible when *x* was at around 0.50, and the structure changed into the one where *B* cations were shifted into the $\langle hhl \rangle$ or $\langle 111 \rangle$ directions, i.e., corresponding to the monoclinic and rhombohedral structures, respectively. These computations gave an explanation for the observed positions of cations inside the oxygen octahedra (Zr and Ti) and cuboctahedra (Pb). Further, they explained qualitatively the experimentally observed changes in lattice parameters and average symmetry. We believe that these results give insight into the observed properties of PZT ceramics, such as high piezoelectric coefficients near the MPB.

Based on neutron powder diffraction data and geometrical considerations, Pb and Ti ion cores are directly responsible for the observed high susceptibility and piezoelectric values of PZT ceramics. The influence of the Zr ion core is indirect in a sense that it creates space for Pb and Ti ions so that they can easily follow the external fields.

ACKNOWLEDGMENTS

We are grateful for Dr. Noheda for many helpful discussions and informing us about their unpublished transmission electron microscope (TEM) results. One of us (J.F.) is grateful to the Vilho, Yrjö ja Kalle Väisälä Foundation, Japan Society for the Promotion of Sciences (Contract No. 13001738), and the Academy of Finland for financial support (Project Nos. 44588, 39189, and 72196).

*Electronic address: jfrantt1@rlem.titech.ac.jp

[1] B. Noheda, D. E. Cox, G. Shirane, J. A. Gonzalo, L. E. Cross, and S.-E. Park, Appl. Phys. Lett. **74**, 2059 (1999).

[2] B. Noheda, J. A. Gonzalo, L. E. Cross, R. Guo, S.-E. Park, D. E. Cox, and G. Shirane, Phys. Rev. B **61**, 8687 (2000).

[3] B. Noheda, D. E. Cox, G. Shirane, R. Guo, B. Jones, and L. E. Cross, Phys. Rev. B **63**, 014103 (2001).

[4] R. Guo, L. E. Cross, S.-E. Park, B. Noheda, D. E. Cox, and G. Shirane, Phys. Rev. Lett. **84**, 5423 (2000).

[5] J. Frantti, V. Lantto, S. Nishio, and M. Kakihana, Jpn. J. Appl. Phys., Part 1 **38**, 5679 (1999).

[6] J. Frantti, J. Lappalainen, S. Eriksson, V. Lantto, S. Nishio, M.

Kakihana, S. Ivanov, and H. Rundlöf, Jpn. J. Appl. Phys., Part 1 **39**, 5697 (2000).

[7] J. Frantti, V. Lantto, S. Nishio, and M. Kakihana, Phys. Rev. B **59**, 12 (1999).

[8] A. G. Souza Filho, K. C. V. Lima, A. P. Ayala, I. Guedes, P. T. C. Freire, J. Mendes Filho, E. B. Araújo, and J. A. Eiras, Phys. Rev. B **61**, 14 283 (2000).

[9] K. C. V. Lima, A. G. Souza Filho, A. P. Ayala, J. Mendes Filho, P. T. C. Freire, F. E. A. Melo, E. B. Araújo, and J. A. Eiras, Phys. Rev. B **63**, 184105 (2001).

[10] D. Vanderbilt and M. H. Cohen, Phys. Rev. B **63**, 094108 (2001).

[11] L. Bellaiche, A. Garcia, and D. Vanderbilt, Phys. Rev. Lett. **84**, 5427 (2000).

[12] J. Kreisel, A. M. Glazer, G. Jones, P. A. Thomas, L. Abello, and G. Lucazeau, J. Phys.: Condens. Matter **12**, 3267 (2000).

[13] J. Kreisel, A. M. Glazer, P. Bouvier, and G. Lucazeau, Phys. Rev. B **63**, 174106 (2001).

[14] A. C. Larson and R. B. Von Dreele (unpublished).

[15] J. Frantti, S. Ivanov, J. Lappalainen, S. Eriksson, V. Lantto, S. Nishio, M. Kakihana, and H. Rundlöf, Ferroelectrics **266**, 73 (2002).

[16] B. Jaffe, W. R. Cook, and H. Jaffe, *Piezoelectric Ceramics* (Academic Press, London 1971), p. 136.

[17] F. Fujishita and S. Hoshino, J. Phys. Soc. Jpn. **53**, 226 (1983).

[18] K. Yamasaki and Y. Soejima, Acta Crystallogr., Sect. B: Struct. Sci. **54**, 524 (1998).

[19] F. Jona, G. Shirane, F. Mazzi, and R. Pepinsky, Phys. Rev. **105**, 849 (1957).

[20] In our previous article, Ref. 6, we erroneously talk about the $Pmm2$ space group in a case when the *a* and *b* axes were rotated by 45°, while the space group used was $Cmm2$.

[21] J. Frantti, J. Lappalainen, S. Eriksson, S. Ivanov, V. Lantto, S. Nishio, M. Kakihana, and H. Rundlöf, Ferroelectrics **261**, 193 (2001).

[22] B. Noheda (private communication).

[23] In their recent work Noheda *et al.* [B. Noheda, L. Wu, and Y. Zhu, Phys. Rev. B (to be published August 2002)] assigned it to the space group Cc. However, NPD data provide no evidence for that symmetry. Particular care must be taken once electron diffraction patterns are interpreted: electron diffraction probes very small volumes of the samples and generally is not suited for an average symmetry determination, especially in a case of small distortions, such as those related to the oxygen octahedral tilts. Further, ion milling is very violent sample thinning technique, which easily generates significant defects. The particle size (in a nanometer scale) they report is not consistent with the superlattice reflections and overall sharp diffraction patterns observed by several groups (including Ref. 3). The explanation that local stresses, due to the cation disorder, generate Cc phase is questionable for the following reason: it is not a well-defined concept (which cations and which type of disorder?) and thus it is difficult to construct a model which would yield numerical values for the phase fractions as a function of temperature and average composition (recalling that this two-phase coexistence is limited to a rather narrow average composition interval, which the model should also explain). We feel that a more natural explanation is provided by the composition fluctuation, which allows one to estimate phase fractions in a quantitative manner.

[24] J. Frantti, S. Eriksson, S. Hull, S. Ivanov, V. Lantto, J. Lappalainen, and M. Kakihana, to be presented in ELECTROCERAMICS VIII–2002 Conference (25–28 August 2002), Rome (unpublished).

[25] H. D. Megaw and C. N. W. Darlington, Acta Crystallogr., Sect. A: Cryst. Phys., Diffr., Theor. Gen. Crystallogr. **31**, 161 (1975).

[26] D. L. Corker, A. M. Glazer. R. W. Whatmore, A. Stallard, and F. Fauth, J. Phys.: Condens. Matter **10**, 6251 (1998).

[27] During the reviewing of the present manuscript there occurred a report by R. Ranjan, S. K. Ragini, D. Pandey, and B. J. Kennedy, Phys. Rev. B **65**, 060102 (2002) assigning a symmetry Pc to the $Pb(Zr_{0.52}Ti_{0.48})O_3$ sample below 210 K. We note that this low-symmetry model predicts tens of reflections not experimentally observed, already in the low 2θ range (only region for which fit, residuals, and Bragg reflection positions are shown, see their Fig. 2). This discrepancy becomes worse as high two-theta range (for which fit, residuals or Bragg reflection positions were not shown in Fig. 1) is considered. This in turn forced the authors to use extraordinary constraints during the refinement (which typically indicates that the symmetry used for the refinement is too low). More recently, an article by D. M. Hatch, H. T. Stokes, R. Ranjan, Ragini, S. K. Mishra, D. Pandey, and B. J. Kennedy, *ibid.* **65**, 212101 (2002), assigning the Cc space group to the low-temperature symmetry of the $x=0.52$ sample, appeared. Inspection of Fig. 1 of this article reveals that the model predicts peaks not experimentally observed, which was the reason why we originally rejected this model in favor of the $R3c$ symmetry. The reflections shown by arrows in their model are describable by the $R3c$ symmetry. As a conclusion, we feel that there was no evidence for the Pc or Cc symmetries, and that there is no further need to speculate on their possible consequences. However, their low-temperature diffraction pattern, including the superlattice reflections, is consistent with the $Cm+R3c$ model.

[28] W. Krans and G. Nolze, computer program POWDERCELL for Windows, Federal Institute for Materials Research and Testing, 1997.

[29] N. W. Thomas and A. Beitollahi, Acta Crystallogr., Sect. B: Struct. Sci. **50**, 549 (1994).

[30] P. M. Woodward, Acta Crystallogr., Sect. B: Struct. Sci. **53**, 32 (1997).

[31] P. M. Woodward, Acta Crystallogr., Sect. B: Struct. Sci. **53**, 44 (1997).

[32] A. M. Glazer, Acta Crystallogr., Sect. B: Struct. Crystallogr. Cryst. Chem. **28**, 3384 (1972).

[33] We use the letter *l* instead of *s* used in the original definition in Ref. 29 to avoid confusion with the *s* parameter defined by Megaw and Darlington (Ref. 25).

[34] G. S. Rohrer, *Structure and Bonding in Crystalline Materials* (Cambridge University Press, Cambridge, England, 2001).

[35] M. O'Keeffe, Acta Crystallogr., Sect. A: Cryst. Phys., Diffr., Theor. Gen. Crystallogr. **33**, 924 (1977).

[36] V. Yu. Topolev and A. V. Turik, J. Phys.: Condens. Matter **13**, 771 (2001).

[37] G. Sághi-Szabó, R. E. Cohen, and H. Krakauer, Phys. Rev. B **59**, 12 771 (1999).

[38] I. D. Brown and D. Altermatt, Acta Crystallogr., Sect. B: Struct. Sci. **41**, 244 (1985).

[39] M. O'Keeffe and N. E. Brese, J. Am. Chem. Soc. **113**, 3226 (1991).

[40] I. D. Brown, A. Dabkowski, and A. McCleary, Acta Crystallogr., Sect. B: Struct. Sci. **53**, 750 (1997).
[41] I. D. Brown, J. Solid State Chem. **90**, 155 (1991).
[42] We corrected a typing error in Table I in Ref. 6: the $z(O_1)$ value of $Pb(Zr_{0.40}Ti_{0.60})O_3$ is 0.0997. Note also that all thermal parameters tabulated in Table III in Ref. 6 must be divided by a factor of 100.
[43] *Handbook of Chemistry and Physics*, 80th ed. (CRC Press, Boca Raton, 1999).
[44] S. A. Ivanov, R. Tellgren, H. Rundlöf, N. W. Thomas, and S. Ananta, J. Phys.: Condens. Matter **12**, 2393 (2000).
[45] R. Comes, M. Lambert, and A. Guinier, Acta Crystallogr., Sect. A: Cryst. Phys., Diffr., Theor. Gen. Crystallogr. **26**, 244 (1970).